IBRACON Structures and Materials Journal
Revista IBRACON de Estruturas e Materiais

ORIGINAL ARTICLE

Effect of duration and pressure of carbonation curing on the chloride profile in concrete

Efeito da duração e pressão da cura por carbonatação do concreto em perfis de cloreto

Roberto Luiz Dias[a]
Neusa Aparecida Munhak Beltrame[a]
Jordi Rius Gonzalez[b]
Ronaldo Alves Medeiros-Junior[c]

[a]Universidade Federal do Paraná – UFPR, Programa de Pós-Graduação em Engenharia Civil – PPEGC, Curitiba, PR, Brasil
[b]Universidade Federal do Paraná – UFPR, Departamento de Construção Civil, Curitiba, PR, Brasil
[c]Universidade Federal do Paraná – UFPR, Centro de Estudos de Engenharia Civil – CESEC, Programa de Pós-Graduação em Engenharia Civil – PPGEC, Curitiba, PR, Brasil

Abstract: Carbonation curing alters the characteristics of the concrete's microstructure and can interfere with the penetration of aggressive ions. The objective of this article was to evaluate the influence of CO_2 pressure and carbonation cure time on chloride profiles. Concrete specimens were cured by carbonation with CO_2 pressures ranging from 5 to 25 Psi, for a time within the carbonation chamber of 8, 24, and 36 hours. These concretes were subjected to 30 wetting and drying cycles in NaCl solution to stimulate the chloride ingress. The carbonation depth and the microstructure of the concrete were monitored over time. Chloride profiles were obtained and modeled by 4 mathematical equations. The results showed that the combination of less time and CO_2 pressure during carbonation curing potentiated the reduction of chloride penetration in concrete. Also, the carbonation curing conditions of 5 and 10 Psi for 8 hours reduced the chloride diffusion coefficient.

Keywords: carbonation curing, CO_2 pressure, curing time, chloride profiles, modeling.

Resumo: A cura por carbonatação altera as características da microestrutura do concreto e pode interferir na penetração de íons agressivos. O objetivo deste artigo foi avaliar a influência da pressão de CO_2 e do tempo de cura da carbonatação nos perfis de cloreto. As amostras de concreto foram curadas por carbonatação com pressões de CO_2 variando de 5 a 25 Psi, por um tempo dentro da câmara de carbonatação de 8, 24 e 36 horas. Esses concretos foram submetidos a 30 ciclos de umedecimento e secagem em solução de NaCl para estimular o ingresso de cloretos. A profundidade de carbonatação e a microestrutura do concreto foram monitoradas ao longo do tempo. Perfis de cloreto foram obtidos e modelados por 4 equações matemáticas. Os resultados mostraram que a combinação de menor tempo e pressão de CO_2 durante a cura por carbonatação potencializou a redução da penetração de cloretos no concreto. Além disso, as condições de cura por carbonatação de 5 e 10 Psi por 8 horas reduziram o coeficiente de difusão do cloreto.

Palavras-chave: cura por carbonatação, pressão de CO_2, tempo de cura, perfis de cloreto, modelagem.

1 INTRODUCTION

Chloride-induced reinforcement corrosion is the main cause of deterioration in reinforced concrete structures located in a marine environment. The formation of expansive ferrous phases from the corrosion of the steel generates

internal stresses and the cracking of the concrete. This process significantly reduces the service life of reinforced concrete structures [1]–[4]. Some techniques have been applied to reduce the penetration of chlorides in the concrete. Among these techniques, Zhang and Shao [5] evaluated the possibility of applying early carbonation curing and observed that this technique can be effective in reducing chloride ingress.

The weathering carbonation process is related to the CO_2 reaction mainly with portlandite in hardened concrete at advanced ages. This reaction reduces the pH of the concrete to approximately 9.0 and can destroy the passivation film of the steel reinforcement [3]. C-S-H is also susceptible to decalcification in the presence of CO_2, producing $CaCO_3$ and silica gel [6].

The early-age carbonation curing differs from weathering carbonation since it is performed in a few hours of hydration, followed by an intentional exposure to high CO_2 concentrations (around 99%) [7], [8]. Carbonation curing has been widespread in the literature to accelerate the increase in compressive strength and reduce the permeability of concrete [5], [8]–[13].

Carbonation curing can produce a controlled depth of carbonation and the drop in pH can be recovered by additional curing in water [14]. According to Zhan et al. [11], resistances in concrete blocks tested after 2 hours of carbonation curing are comparable to 6 hours of steam curing. Zhang and Shao [8] found that the absorption of 16% CO_2 by cement content can reduce the pH of the concrete to about 9.2 on the surface. However, the subsequent hydration can raise the surface pH to approximately 12.5 [10], decreasing the risk of steel corrosion due to carbonation in this case.

CO_2 introduced early in the concrete reacts with non-hydrated clinker (especially C_2S and C_3S), $Ca(OH)_2$, and C-S-H. The main phases formed are amorphous $CaCO_3$, C-S-H with less Ca/Si ratio, and silica gel [15], [16]. However, the C-S-H content, the Ca/Si ratio, and the degree of crystallization of $CaCO_3$ increase with the subsequent hydration in water [16]. The $CaCO_3$ generated in the capillary pore walls by carbonation cure leads to a reduction in the larger capillary pores and a denser microstructure, acting as an external shield against external ions [5], [8], [17], [18]. The reduction in the permeability of concrete is due to the formation of a greater amounts of solid phases [7], [8], [16].

Chen and Gao [19] identified that the carbonation cure can considerably influence the pore structure of the cement paste. The superficial (carbonated) region of the specimens had much lower porosities in relation to the internal layers. The proportion of small capillary pores (25 to 1000 nm) decreased, while the large capillary pores (from 1000 nm) increased with the advancing depth of the samples. Besides, total porosity was reduced by 40% in the study by Zhang and Shao [20]. The size of the dominant capillary pores before carbonation curing was 10 to 50 nm and decreased to less than 10 nm after this type of cure. This indicated that carbonation curing can effectively refine the pore structure.

There are two essential influences of carbonation curing on the properties of concrete: (i) the increase in compressive strength and the reduction of water absorption at an early age; and (ii) the changes caused in the microstructure of the concrete due to calcium carbonate precipitation, thus improving performance and durability [21]. This research will focus on the second (resistance to chloride penetration). The variation in compressive strength and water absorption has not been evaluated since this influence has already been excessively addressed in the literature [7], [9], [10]-[13], [22].

Several studies have demonstrated changes in the durability of cement composites in terms of different degradation mechanisms due to carbonation curing. The carbonation cure contributed to the reduction of porosity, permeability, and ettringite formation [10], [16], [23]-[25]. Also, the carbonation cure increased the resistance to attack by external sodium and magnesium sulfates [15], [22], [26], acids [17], carbonation by weathering [5], damage from freeze-thaw [22], drying shrinkage [11], [27], [28], and penetration of chloride ions [5], [16], [20]. The main applications for carbonation curing are related to the production of precast concrete and concrete blocks [23], [27], [28].

The main conclusions of the studies about improving the durability of carbonation-cured concrete are related to the reduction in $Ca(OH)_2$ content on the concrete surface and the decrease in the C_3A content after carbonation curing, making them less vulnerable to the chemical attack of aggressive agents [9], [12], [22]. Zhang and Shao [5], [20] demonstrated that CO_2 curing reduced by 50% and 60% the total and free chloride content of concretes, respectively. Increased resistance to chloride migration has also been reported by Pan et al. [16]. This effect was attributed to the superficial protective layer rich in carbonates, less permeable, less absorptive, and with a comparable pH value. However, these studies applied only one level of CO_2 pressure and carbonation cure time. The main research question of this study is whether the protection remains efficient with the alteration of these parameters.

Although the early carbonation cure technique is widely discussed in the literature, the lack of standardization has led to the adoption of different parameters of time and CO_2 pressure among researchers. The reaction rate of the carbonation cure is mainly controlled by CO_2 diffusion, which can be influenced by the time, concentration, and pressure of the CO_2 gas. Table 1 summarizes some research on carbonation curing with different pre-cure procedures, CO_2 concentration, duration, pressure and subsequent cure.

Rev. IBRACON Estrut. Mater., vol. 16, no. 6, e16603, 2023

2/17

Table 1: Some recent durability studies concerning carbonation curing.

| Ref. | Test samples | Pre-cure | Carbonation | | | Post-cure |
			CO$_2$ (%)	Pressure (Psi)	Time (h)	
[29]	PC paste	18 h sealed and 3 h (2 ± 1) ºC, 50% RH	99.5	14.50	1, 2, 3, 4, 24, and 72	28 days in water
[15]	PC paste	24 h in mold, (20 ± 3) °C	20.0	--	4	28 d, (20 ± 3) °C, RH 90%
[25]	PC Concrete block	4 h, (23 ± 2) ºC, 60% RH	10	--	20	27 days, (23 ± 2) ºC, 95% RH
[16]	PC mortar	24 h in sealed mold, (20 ± 1) °C, RH ≥ 98%	99.0	29.00	3 and 6	28, 90 and 180 days immersed in water
[20]	PC concrete and cement paste	5 h in mold, 5-6 h 25 °C, RH 50%	99.8	72.52	12	27 days, 25 °C, 95% RH
[24]	PC paste	24 h in mold, 20 °C	10	14.69	672	--
[23]	PC mortar	6 h, 26 ºC, (50 ± 5) % RH	99.0	10.00	12	28 days, sealed and sprinkling water
[9]	PC mortar and concrete	0-6 h, 22 °C, RH 60%	99.5	29.00	3	27 days immersed in water, 22 ºC
[30]	PC mortar and paste	24 h, 20 °C	5	14.69	168, 336, 672	--
[10]	PC paste and steel slag	7 days, (23 ± 2) ºC, 98% RH and 2 days 30-40% RH	99.9	14.69	24, 72, and 336	--
[28]	PC block concrete	6h, 50% RH, 25 ºC	99.5	1.45 to 72.52	1, 2, 3, 6, 18, and 24	28 days air
[12]	PC concrete	5 h in the mold and 5.5 h in 25 °C and (50 ± 5) % RH	99.8	72.52	2, 12, and 24	1, 4, 28, 90, 180, and 360 days, 25 °C, 95% RH
[5]	PC Concrete	5-6 h in mold, 5.5 h 25°C, RH (50 ± 5) %	99.8	72.52	12	27 days, 25 °C, 95% RH
[31]	PC paste and reactive MgO	(24 ± 2) h, (23 ± 2) ºC, 90% RH in mold and 24 h, vacuum	99.9	14.69	168, 672, and 1344	--
[22]	PC concrete	18 h, 25 °C, RH 60%	99.5	21.75	2	27 days sealed and sprinkling water
[27]	Cement block concrete	3-6 h in the mold and 4 h out of the mold	Not indicated	10.00	2	--
[17]	Cement block concrete	2 h and 4 h steam (40-63 °C)	99.5	21.75	2	27 days sealed
[26]	PC paste	4 h, 65 ºC, and 100% RH; 8 h autoclave (180 ºC)	5	--	672	--

The objective of this article was to investigate the effect of duration and pressure of carbonation curing on chloride profiles. Concrete specimens exposed to 30 wetting and drying cycles of NaCl (3.5%) solution were investigated after carbonation curing with pressures ranging from 5, 10, 15, 20, and 25 Psi, and durations of 8, 24, and 32 hours. A reference concrete (conventional curing) was used to compare the results.

The main innovation of this article is in the determination of chloride profiles for concrete cured by carbonation at different levels of CO$_2$ pressure and curing time. In addition, the profiles were modeled to calculate the diffusion coefficient and the chloride surface concentration for a quantitative evaluation of the results. No article has been found in the literature by these authors that use this approach. Therefore, the results of this article can certainly contribute to the advancement of knowledge on this topic.

2 MATERIALS AND EXPERIMENTAL PROGRAM

Concrete specimens were molded for carbonation curing at different CO$_2$ pressures and for different times, in addition to the reference concrete (submerged curing in water). These specimens were subjected to wetting and drying cycles in chloride solution for 30 weeks (210 days). After this period, the chloride profiles were determined and modeled from 04 different chloride models available in the literature.

Rev. IBRACON Estrut. Mater., vol. 16, no. 6, e16603, 2023

3/17

2.1 Materials and concrete production

Brazilian Portland cement CP-II F 32 (equivalent to Portland-limestone cement CEM II / A-L 32.5N) was used. Table 2 shows the characterization of this cement. The fine aggregate was natural river sand with specific gravity of $2.67g/cm^3$, bulk density of $1.52g/cm^3$, water absorption of 0.95%, fineness modulus of 2.41, and maximum aggregate size of 4.8 mm. The coarse aggregate was basaltic gravel with maximum aggregate size of 9.5 mm, specific gravity of $2.76g/cm^3$, bulk density of $1.55g/cm^3$, and water absorption of 0.81%.

Cubic concrete specimens were produced (100 mm edge). The proportion of materials (by mass) of the concrete was 1: 1.6: 2.5 (cement: sand: gravel) with a water-to-cement ratio of 0.50. The concrete had a cement content of 416 kg/m^3, consistency (slump test) of (100 ± 20) mm, and a specific gravity of 2,420 kg/m^3. Therefore, a conventional concrete mix was chosen. No chemical additive (superplasticizer) was used in this research. Only a concrete mixture was evaluated since this article focuses on assessing the effect of pressure and duration of carbonation cure in chloride penetration. The effect of the water-to-cement ratio and other types of binders (including pozzolans) on carbonation cure and chloride ingress is well defined in the literature.

Table 2. Characterization of the Portland cement.

Property	Unit	CP-II F	Property	Unit	CP-II F
CaO	%	59.51	Specific gravity	g/cm^3	3.03
SiO_2	%	16.80	Initial setting time	h:min	03:40
Al_2O_3	%	3.86	Final setting time	h:min	04:30
MgO	%	3.13	Fineness Blaine	cm^2/g	3,730
SO_3	%	2.56	# 200	%	0.80
Fe_2O_3	%	2.56	# 325	%	6.70
Loss on ignition	%	10.44	Compressive strength (3 d)	MPa	29.8
Free CaO	%	0.70	Compressive strength (7 d)	MPa	35.2
Insoluble residue	%	0.75	Compressive strength (28 d)	MPa	40.8
Alkaline content (Na_2O and K_2O)	%	0.61			

Five CO_2 pressures inside the carbonation chamber (5, 10, 15, 20, and 25 Psi), and three different carbonation curing times (8, 24, and 32 hours) were used. These parameters were chosen after an extensive literature review on the range of pressures and carbonation cure times applied in other studies. In addition to these carbonation curing parameters, a conventional water curing was also performed on reference concretes (three specimens). These reference specimens were casted and were not subjected to carbonation curing, only chloride penetration. Table 3 shows the codes used to represent the concrete samples.

The concrete specimens were casted according to the NBR 5738 [32] standard. The compressive strength of concrete was (27.8 ± 1.24) MPa at 28 days. The compressive strength was performed only at 28 days to characterize the concrete. The variation in compressive strength during carbonation curing was not evaluated, since several studies in the literature have already done this investigation [7], [11], [13], [14].

Table 3. Carbonation cure parameters used in this research.

Code	Pressure (Psi)	Time (h)	Code	Pressure (Psi)	Time (h)
5p8h	5	8	20p8h	20	8
5p24h	5	24	20p24h	20	24
5p32h	5	32	20p32h	20	32
10p8h	10	8	25p8h	25	8
10p24h	10	24	25p24h	25	24
10p32h	10	32	25p32h	25	32
15p8h	15	8	REF	-	-
15p24h	15	24			
15p32h	15	32			

2.2 Concrete curing

The conventional water curing of the reference concrete was executed for 28 days. The carbonation curing process was developed in four stages: step 1 - mold curing (6 hours); step 2 - pre-cure (18 hours); step 3 - cure within the

carbonation chamber (8, 24, and 32 hours); and step 4 - subsequent hydration (27 days). Figure 1a shows the representation of each of these steps.

2.2.1 Step 1 - mold curing

Soon after mixing and placing the concrete in the forms, the surface of the specimens was protected with plastic film and the concretes remained in a laboratory environment for 6 hours. This period was defined based on the final setting time of the cement (04 hours and 30 minutes, according to Table 2). Therefore, a time slightly longer than the final setting time was determined to ensure that the concretes do not break during their removal from the forms.

2.2.2 Step 2 - pre-cure

After step 1, the concretes were removed from the forms and remained in a climatic room (temperature = 25 ± 1 °C; and relative humidity = 50 ± 5%) for 18 hours. This step allows part of the free water inside the concrete to evaporate, leaving more space for the carbon dioxide to penetrate since excess water can block the diffusion of CO_2 generating a limitation in the carbonation reaction [8]. The concrete mass was determined before and after step 2 on an electronic scale with an accuracy of 0.01 g. The water loss of the concretes during the 18 hours of pre-curing was 50.43%. El-Hassan et al. [33] and El-Hassan and Shao [34] found a value of water loss of 51% for the same period.
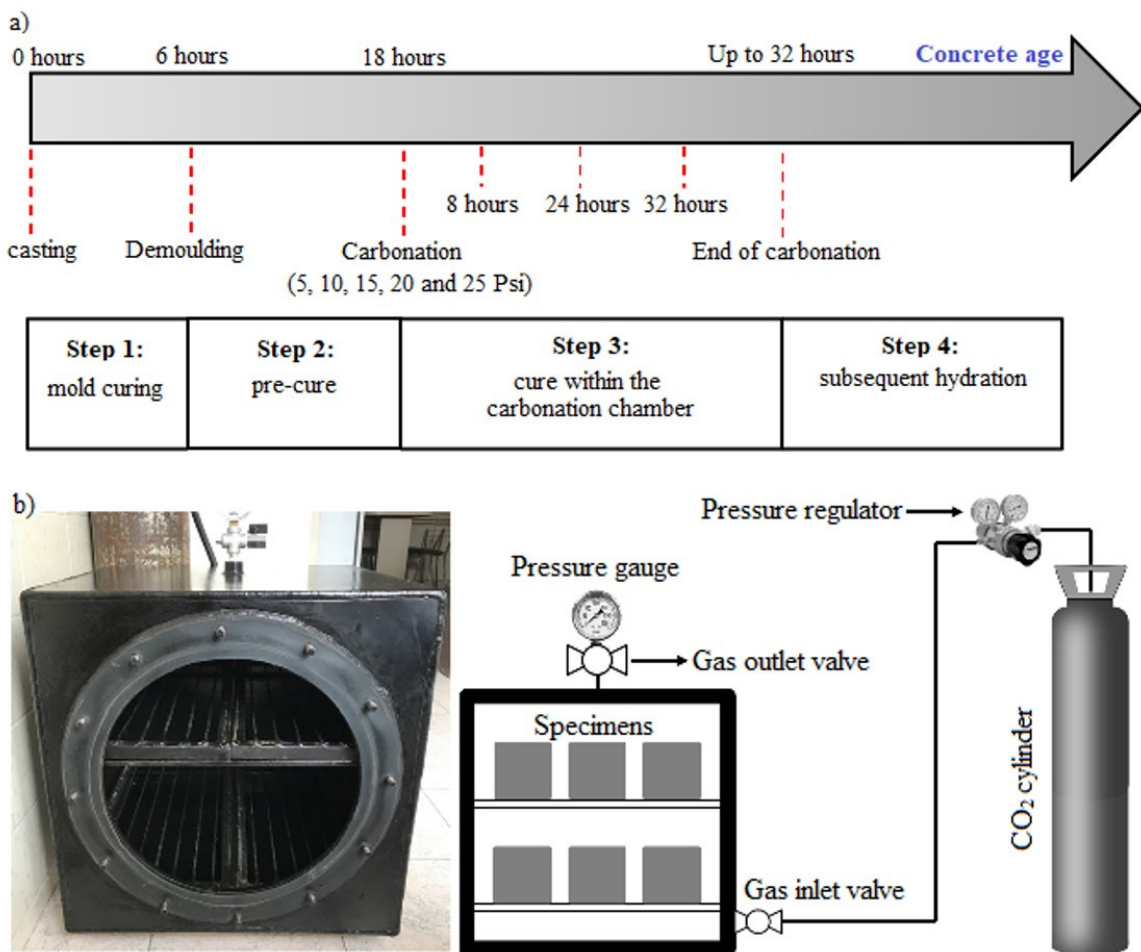

Figure 1: Illustrative schemes showing: (a) carbonation curing steps; (b) carbonation chamber operating system.

Rev. IBRACON Estrut. Mater., vol. 16, no. 6, e16603, 2023

5/17

2.2.3 Step 3 - cure within the carbonation chamber

The concrete specimens were inserted into the carbonation chamber at this step (Figure 1b). CO_2 with a purity of 99.5% was used, based on the studies by Rostami et al. [17], Abdullahi et al. [35], and Zhan et al. [11]. Two pressure gauges were installed in the chamber. The first served to monitor the pressure of the tank, and the second to indicate the outflow of the gas. Therefore, the internal pressure of the gas was controlled within the pre-defined values (5, 10, 15, 20, and 25 Psi).

Before injecting CO_2, the carbonation chamber was aspirated using a vacuum pump. This process was executed to ensure that the chamber would be fully occupied by CO_2 gas. After this process, the injected CO_2 and the pressure inside the chamber were regulated to remain constant, ensuring a continuous supply of the gas to the equipment throughout the carbonation period.

The concrete specimens remained for 8, 24, or 32 hours inside the carbonation chamber, depending on the desired curing time. Seven specimens were used for each curing time. From these seven specimens, two were used to determine the carbonation depth immediately after step 3, two were used to determine the carbonation depth immediately after step 4, and the remaining three specimens were used in the chloride penetration test. Figure 2 shows a schematic illustrating these procedures.
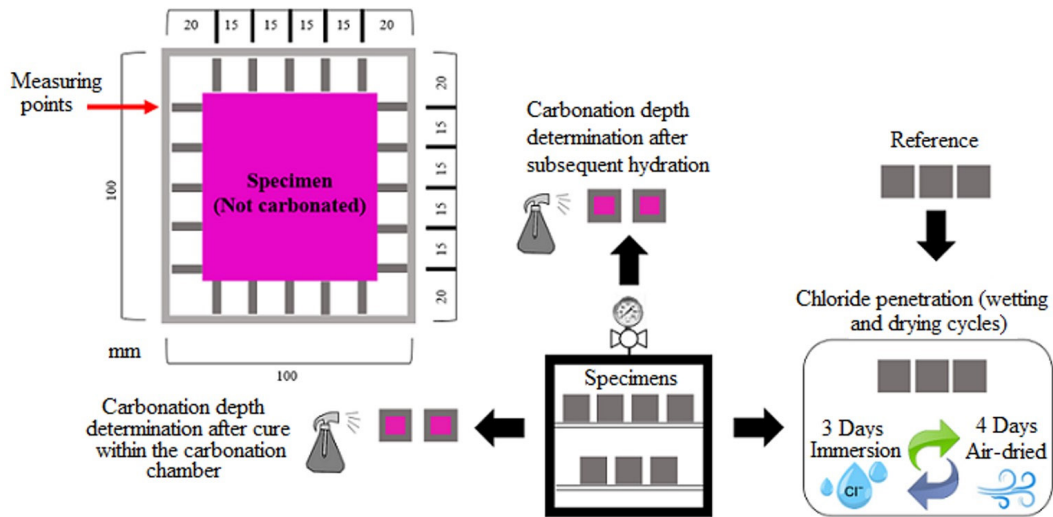

Figure 2. Distribution of specimens subjected to carbonation curing.

The specimens were weighed again immediately after step 3. Then, the increase in concrete mass was calculated from Equation (1) [8], [33] during the period inside the carbonation chamber. This measure compares the mass of the samples before and after the period inside the carbonation chamber, and indirectly estimates the capture of carbon dioxide (Ab_{CO_2}) in the concrete, according to [33].

$$Ab_{CO_2}(\%) = \frac{M-m}{M_{cem}} \tag{1}$$

Where M is the mass after the period inside the carbonation chamber; m is the mass of the concrete after the pre-curing step; and M_{cem} is the mass of the cement.

2.2.4 Step 4 - subsequent hydration

The subsequent hydration step is recommended by several studies regarding carbonation cure [5], [12], [36] to ensure an additional hydraulic reaction to cement grains that did not react during the first hours of casting. Therefore, the specimens were immersed in a lime-saturated water solution for 27 days after step 3 [9]. Thus, the total curing period was 28 days, which comprises 1 approximate day of carbonation curing (8, 24, or 32 hours), and 27 days of subsequent hydration.

2.3 Carbonation depth determination

The carbonation depth was determined using a phenolphthalein colorimetric indicator solution, according to RILEM CPC 18 [37]. A solution of 1% phenolphthalein, 29% distilled water and 70% alcohol was sprayed on the newly broken concrete surfaces. The specimens were broken longitudinally using a press. Twenty measurements (Figure 2) on each side of the specimens were made with a digital caliper with a precision of 0.01 mm.

2.4 Chloride penetration

After the curing steps (approximately 28 days), the concrete specimens were subjected to wetting and drying cycles in an aqueous solution with 3.5 wt.% sodium chloride (NaCl). For this purpose, the samples were initially sealed on four sides with waterproof epoxy resin to enable the unidirectional penetration of the chlorides. Each cycle lasted 7 days (three days of total immersion in chloride solution and four days air-dried). During the initial three weeks of testing, the masses of the specimens were measured and the absorption of the solution recorded for permeability characterization. The chloride profiles were determined after 30 complete wetting and drying cycles (210 days). The choice of the number of cycles was made in order to extend the experimental program as long as possible to performed this research, considering issues of logistics, production, cost, storage, and time available for the tests.

The determination of chloride concentrations in concrete was executed using the titration method, according to RILEM TC 178-TCM [38]. This method involves titrating the silver ion in an acid medium with a standard solution of ammonium thiocyanate (NH_4SCN) and the Fe^{3+} ion as an indicator. The precipitate is formed with an excess of standard silver nitrate solution $AgNO_3$.

The concrete samples were taken from the cubic specimens using a circular saw. The dry cut was performed in 4 slices, every 10 mm from the surface of the samples. The concrete slices were crushed using a pan mill to obtain the powdered concrete sample (> 0.16 mm). The powder samples were homogenized to guarantee a representative profile and allow an accurate determination of the chloride content by the chemical procedure, analyzed by titration using an ammonium thiocyanate solution [38]. Three specimens were used for each curing condition (Table 3) applied in this research.

After determining the chloride profiles, the chloride penetration was modeled to estimate the chloride diffusion coefficient and the chloride surface concentration. To increase the reliability of the conclusions, four different models available in the literature were used. The models used were the resolution of the error function of Fick's second law (Equation 2) [39], the modified Holliday equation (Equation 3) [40], [41], the FIB 34 model (Equation 4) [42], and the EHE-08 equation (Equation 5) [43]. The modified Holliday equation can model the peak region of chloride penetration in concrete, while the other three equations model only the chloride diffusion. These models are widely applied in the literature to estimate the penetration of chlorides in concrete [36], [40], [44]–[48]. The adjustment by the least-squares method was applied, considering only the period of diffusion of the chloride profiles for Equations 2, 4, and 5 and the entire profile for Equation 3.

$$C(x,t) = Cs \cdot \left[1 - erf\left(\frac{x}{\sqrt{4.D.t}}\right)\right] \tag{2}$$

$$C(x,t) = \frac{1}{\frac{1}{R1}\left[1 + \frac{(x-R3)^2}{(D.t)}\right]} \tag{3}$$

$$C(x,t) = (Cs, \Delta x) \cdot \left\{1 - erf\left(\frac{x - \Delta x}{2.\sqrt{D.t}}\right)\right\} \tag{4}$$

$$C(x,t) = Cs \cdot \left\{1 - \frac{x}{\sqrt{12.D.t}}\right\}^2 \tag{5}$$

Where C(x,t) = chloride concentration (%) at depth x and time t; Cs = surface chloride concentration (%); *erf* = Gauss error function; *x* = chloride penetration depth (cm); *D* = chloride diffusion coefficient (cm^2/s); *t* = time (s); R_3 = Δx = depth of the convection zone (cm); R_1 = Cs,Δx = chloride concentration (%) at the depth Δx.

Rev. IBRACON Estrut. Mater., vol. 16, no. 6, e16603, 2023

7/17

2.5 Microstructure and statistical analysis

Samples of the concrete specimens were extracted at two depths (external and internal) to determine the microstructure analysis. The depth designated as external consisted of the samples in a range of 0-10 mm from the surface. This region was expected to be carbonated after carbonation curing. The depth designated as internal consisted of the samples 50 mm away from the surface (core of the specimen and therefore not carbonated).

Cubic samples with an edge of approximately 1 cm were extracted from the specimens for Scanning Electron Microscopy (SEM) analyses associated with X-ray Dispersive Energy Spectroscopy (EDS). The equipment used was the Tescan Mira 3 Microscope with SE/BSE backscattered detectors and the Oxford X-MaxN 50 X-ray Analytical Probe. The samples were sputtered with gold.

The statistical analysis of the results was made from the analysis of variance (ANOVA). ANOVA consists of comparing two factors (Fcalculated and Ftabulated). If the Fcalculated value is higher than the Ftabulated, the influence is considered significant. A 95% confidence level was used. Then, the significant means were compared using the Tukey test.

3 RESULTS AND DISCUSSIONS

3.1 Chloride profiles and modeling of chloride penetration

Table 4 summarizes the carbonation depth and mass increment obtained after carbonation curing, varying the carbonation time and pressure. In addition, the solution absorption rates during the sodium chloride immersion test are also displayed. In general, the longest carbonation time produced the greatest depths of carbonation and mass addition, ranging from 9.42 to 22.54 mm and from 6.46 to 15.19%, respectively. The rates of absorption of the NaCl solution found were 4.1% to 6.6%, depending on the duration and CO_2 pressure.

The results of the chloride profiles were evaluated in two ways. Firstly, the effect of CO_2 pressure on the chloride profile will be discussed. Later the profiles will be evaluated focusing on the effect of carbonate curing time. Finally, the chloride diffusion coefficients will be discussed based on the modeling of the chloride profiles.

Table 4. Sample properties after initial carbonation cure.

Pressure	Depth of carbonation (mm)			Mass increment CO_2 (%)			Absorption (%)		
	8 h	24 h	32 h	8 h	24 h	32 h	8 h	24 h	32 h
5 Psi	11.63	17.51	22.54	6.46	11.48	15.19	4.1	5.2	4.9
10 Psi	9.42	14.65	20.52	7.55	10.42	11.56	5.3	6.6	6.0
15 Psi	12.92	21.58	20.57	6.98	13.01	13.63	4.5	4.8	6.2
20 Psi	13.92	17.87	22.43	7.76	10.37	10.97	4.3	6.0	6.4
25 Psi	14.87	20.44	21.87	8.43	10.97	12.44	5.1	5.4	6.1

Carbonation-cured concrete generally had a lower total chloride content compared to reference concrete (Figure 3). This reduction occurred in all specimens at the first depth (until 10 mm). In the innermost depths (mainly after 20 mm), some concentrations of chlorides in the carbonated concrete were higher than the reference concrete. Zhang and Shao [5] observed that the reduction in chloride concentrations due to carbonation cure is more intense in the first 25 mm. According to these authors, carbonation-cured concrete had chloride contents more than 50% lower than reference concrete. It should be noted that Zhang and Shao [5] did not vary the time and CO_2 pressure, unlike the present article.

The lower concentration of chlorides in the most superficial depths of carbonated concrete is related to the extensive formation of calcium carbonate which physically hinders the initial penetration of chlorides into the concrete during the wetting and drying cycles. This phenomenon occurs due to the structure of the pore network modified by carbonation. In this case, the carbon dioxide precipitate as $CaCO_3$ and mixed with C-S-H gel, resulting in a structure with less permeability in the first layers. The effect of reducing permeability and increasing the compressive strength of concrete cured by carbonation has been confirmed in several studies [7], [22], [10]–[13], [49], [50]. In the innermost depths, the effect of carbonation cure on concrete is less intense, or nonexistent for depths greater than 25 mm.

The greatest reduction in the chloride profiles of carbonated concretes in comparison with the reference concrete occurred for the curing time of 8 hours (Figure 3a). Therefore, using a shorter curing time was more efficient to increase the resistance of the concrete to chloride penetration. According to Table 4, keeping the pressure constant, the lowest absorption (%) occurred for the shortest curing time (8 hours). Also, from 15 Psi onwards, curing for 32 hours also caused greater absorption than curing for 24 hours.
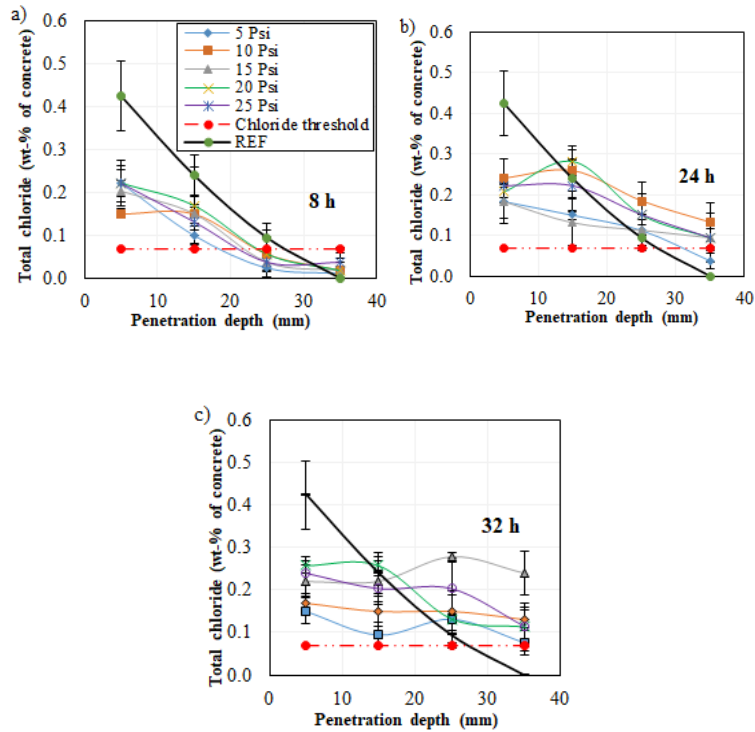
Rev. IBRACON Estrut. Mater., vol. 16, no. 6, e16603, 2023

8/17

Figure 3. Effect of pressure on the chloride profile: (a) 8 h; (b) 24 h; (c) 32 h

According to Figure 3, the effect of CO_2 pressure on chloride profiles increases with the curing times, and this effect was negative as the CO_2 pressure increases. The chloride profiles with the different pressure levels drifted away with increasing curing time. Furthermore, increasing the pressure can reduce the concrete's resistance to chloride ingress mainly for the curing time of 32 hours. Only the application of the curing time of 8 hours made it possible to reduce the chloride profiles (regardless of pressure) to practically all depths. Therefore, the combination of less time and pressure during carbonation curing potentiated the reduction of chloride penetration in concrete.

Figure 3 also shows the setting of a 0.07 (wt.% concrete) chloride threshold, which is equivalent to 0.40 (wt.% cement). The conversion of the chloride content units was performed using Equation 6 [43]. This is the most widely used value in the literature to assess the chloride threshold for the onset of chloride-induced corrosion [43], [48], [51]. Considering a concrete cover of around 35 mm, only the carbonation cure applied for 8 hours would be able to protect the reinforcement against corrosion regardless of the CO_2 pressure (Figure 3a).

$$Cl(wt \cdot \% \ cement) = Cl(wt \cdot \% \ concrete) \cdot \left(\frac{M_c}{k}\right) \tag{6}$$

Where Cl is the chloride concentration; Mc is the concrete specific gravity; and k is the cement content in concrete. Equation 6 suggests Mc equal to 2,300 kg/m^3 in its original equation from [43]. However, the concrete specific gravity obtained experimentally (= 2,420 kg/m^3) was applied in this article.

According to Figure 4, there is a tendency for the chloride profiles to become higher than the reference concrete with increasing pressure. This reinforces the hypothesis of increasing the CO_2 pressure does not seem to be an adequate solution for the protection of the carbonation-cured concrete against chloride penetration. Moreover, Figure 4 clearly shows that increasing the curing time does not reduce chloride ingress.

The chloride profiles were modeled to quantitatively assess the chloride penetration in the different concrete mixtures. The chloride profiles were modeled considering the total chloride content in wt.% cement (instead of wt.%

concrete) to facilitate the comparison of the results of diffusion coefficients and surface chloride concentrations with the literature. The conversion of the chloride content units was performed using Equation 6.
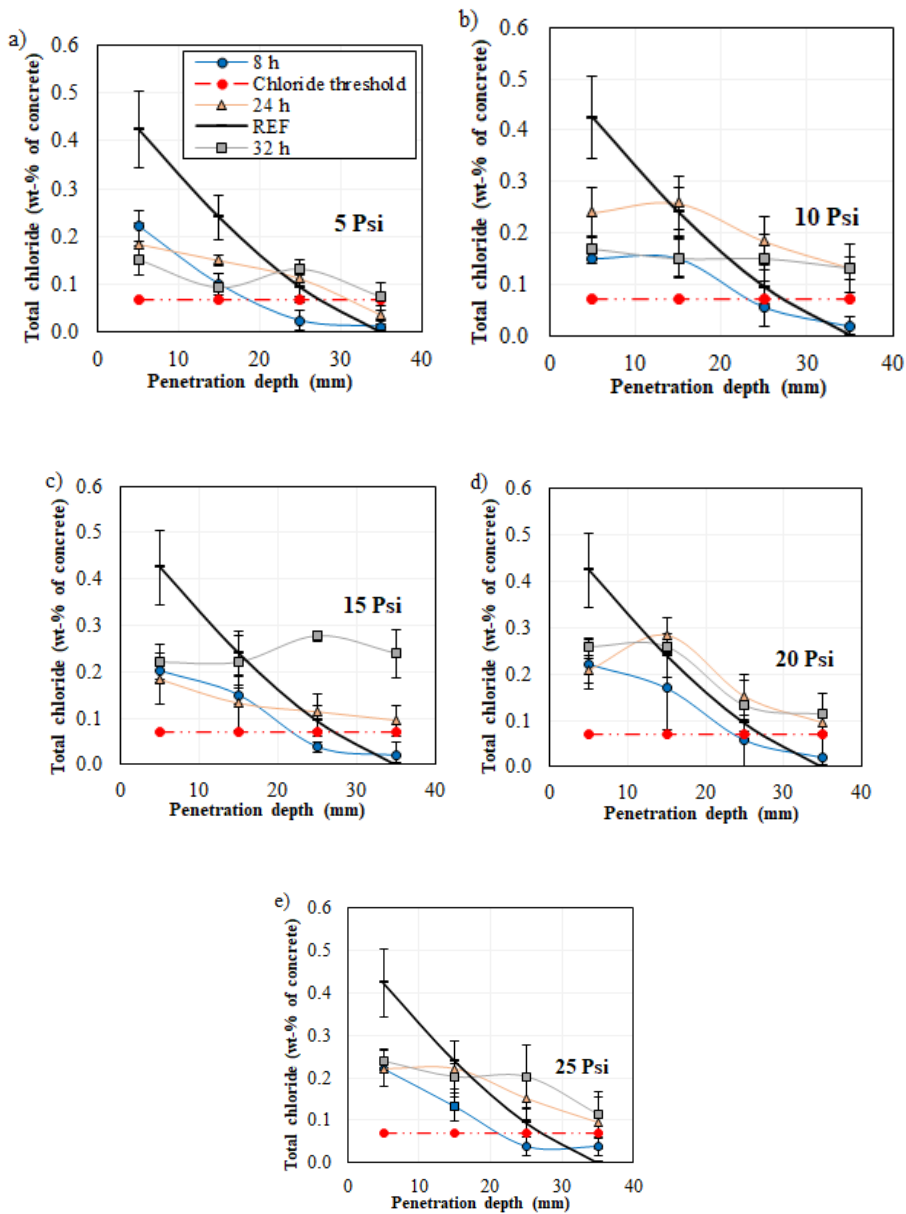

Figure 4. Effect of carbonate curing time on the chloride profile: (a) 5 Psi; (b) 10 Psi; (c) 15 Psi; (d) 20 Psi; (e) 25 Psi.

Figures 5-8 show the estimated chloride diffusion coefficient (D), the surface chloride concentration (Cs), and the determination coefficients for each profile. There was no significant variation between the modeling curves for the different equations. However, Holliday's equation showed the advantage of being able to model the convection zone, and consequently, estimate the surface concentration of chlorides in the concrete. The four equations applied in this research were able to satisfactorily model almost all chloride profiles. It was not possible to model efficiently the 15p32h concrete (Figure 8c) since this profile did not clearly show the distinction of the convection and diffusion zone. In this case, only the last two points could be used for the diffusion models (Equations 2, 4, and 5). However, the behavior of this profile was simulated using Holliday's modified equation.
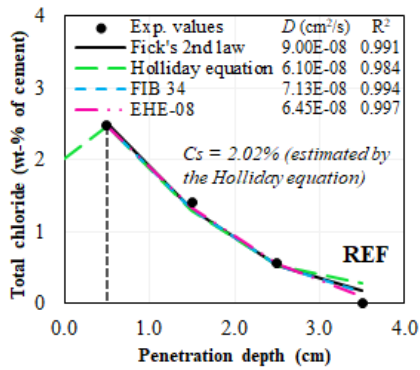
Rev. IBRACON Estrut. Mater., vol. 16, no. 6, e16603, 2023

10/17

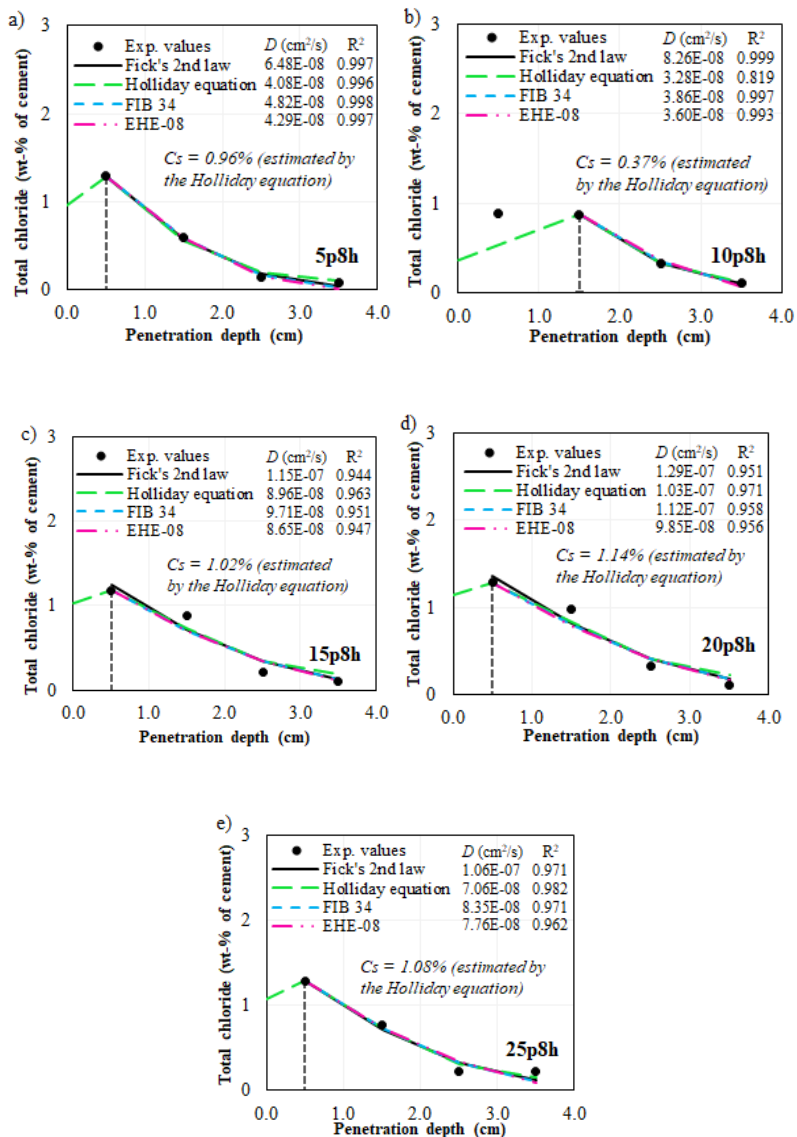**Figure 5.** Modeling of chloride penetration – reference concrete.

Figure 6. Modeling of chloride penetration curing time of 8 h: (a) 5 Psi; (b) 10 Psi; (c) 15 Psi; (d) 20 Psi; (e) 25 Psi.
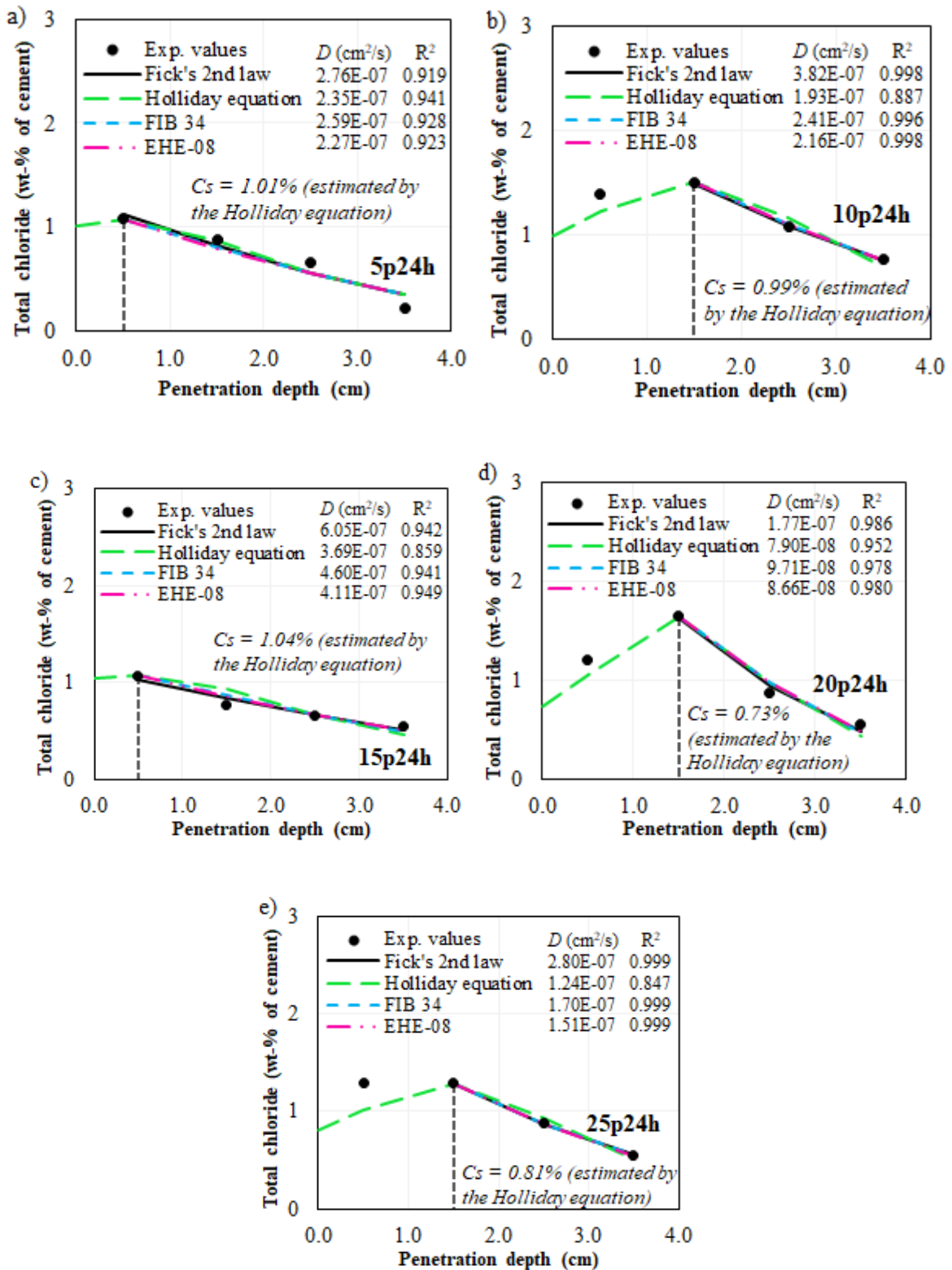
Figure 7. Modeling of chloride penetration – curing time of 24 h: (a) 5 Psi; (b) 10 Psi; (c) 15 Psi; (d) 20 Psi; (e) 25 Psi.
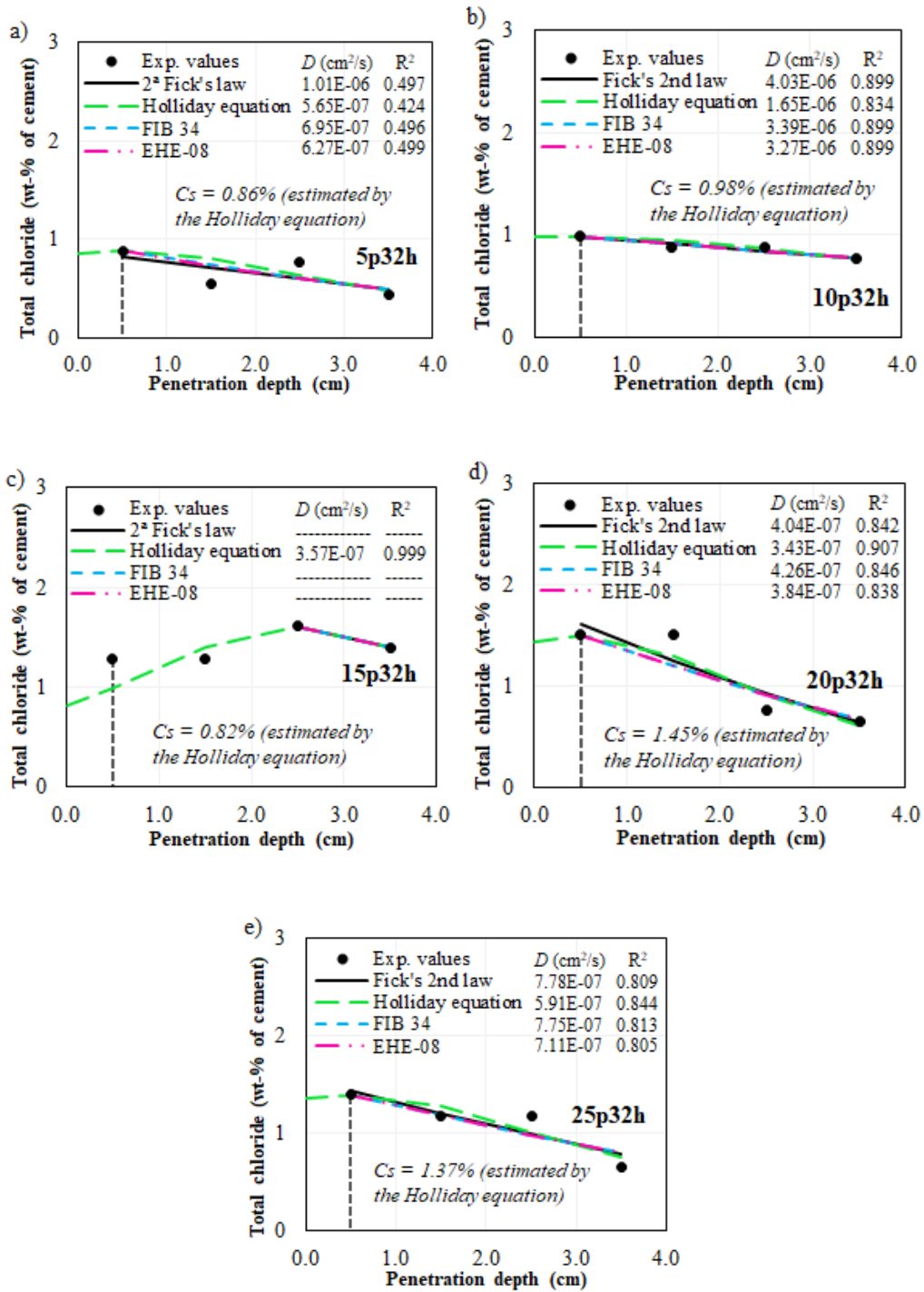
Figure 8. Modeling of chloride penetration – curing time of 32 h: (a) 5 Psi; (b) 10 Psi; (c) 15 Psi; (d) 20 Psi; (e) 25 Psi.

The action of wetting and drying cycles created a convective zone in the chloride profiles. According to Figures 5-8, CO_2 pressure and carbonation curing time did not influence the depth of the convection zone. This zone was around 5 to 15 mm. Ye et al. [52] also found convection zones at depths ranging between 5 and 15 mm when modeling the chloride penetration into cracked concretes subject to drying and wetting cycles.

Rev. IBRACON Estrut. Mater., vol. 16, no. 6, e16603, 2023

13/17

At the depth of the convective zone, the drying period of the wetting and drying cycles produces a highly concentrated pore solution of chloride ions, which can be transported quickly into the cementitious matrix, due to capillary suction during the subsequent wetting period. The depth of the convection zone is mainly influenced by the depth of the concrete's moisture variation during the wetting and drying cycles. According to [52], this humidity variation is related to the concrete exposure surface. Therefore, this parameter was less affected by carbonation curing, since the concrete exposure surface is the same regardless of the curing condition.

The diffusion coefficient of the reference concrete was between 6.10E-08 and 9.00E-08 cm^2/s. These values are coherent and similar to the coefficients found in different studies for conventionally cured concretes [4], [48], [51]. The carbonation curing conditions of 5 and 10 Psi for 8 hours were the only ones that reduced the chloride diffusion coefficient compared to the reference concrete. According to Figures 5 and 6, the concretes cured in the other three pressure levels (15, 20, and 25 Psi) for 8 hours had diffusion coefficients similar to the reference concrete, with values between 7.76E-08 to 12.9E-08 cm^2/s. However, the estimated chloride surface concentration for all concretes cured for 8 hours in the carbonation chamber was lower than the reference concrete. Thus, the carbonation cure applied over 8 hours was efficient to increase the concrete's resistance to chloride penetration. The use of four different models generated ranges of diffusion coefficient (and not a single value), increasing the reliability of the discussions of these results.

The chloride profiles became more horizontal with increasing CO_2 pressure and time. This means that the values of the diffusion coefficients have increased. However, the surface chloride concentration of all concrete mixtures cured by carbonation was lower than the reference concrete. Therefore, chlorides had greater difficulty in initially entering concrete cured by carbonation, due to the higher density of the surface layers of the cementitious matrix related to the formation of calcium carbonate. The capillary pores of the concrete are partially filled and blocked due to the deposit of calcium carbonate ($CaCO_3$). Thus, the intensity of capillary suction is decreased due to a reduction in capillary porosity on the surface and the loss of connectivity between pores within the concrete, as showed by [5], [19], [53]. Therefore, the chloride content in carbonated concrete samples is lower in the surface region.

However, once inside the concrete, chlorides had greater mobility in concrete cured by carbonation at high pressures during the longest times. This behavior is related to the greater difficulty of carbonated concrete to chemically fix chloride ions for the formation of Friedel's salt. In this study, Friedel's salt was easily found in the reference concretes in the first depth of analysis (0-10 mm) after exposure to thirty weeks of wetting and drying cycles in chloride solution. However, the identification of this salt was more difficult (it required more samples and more time for analysis) and in a smaller amount for carbonation-cured concretes (Figure 9), in addition to occurring in more internal depths (between 25-35 mm). The confirmation of Friedel's salt was performed through EDS and stoichiometric calculations.

The chemical bonding capacity of chlorides with the hydrated cement phases for the formation of Friedel's salt is related to the content of aluminates in the cement composition [54]. The results of this article indicate that Friedel's salt is more unstable in carbonated concrete, mainly due to the pH reduction caused by carbonation, similarly to other studies that evaluated the interaction between carbonation and chloride ingress [3], [44], [53]. Therefore, depending on the CO_2 pressure and curing time during carbonation curing, concrete may be less resistant to chloride-induced corrosion. For these cases, although the surface concentration of chlorides is less than a conventionally cured concrete (reference), the chlorides can reach the concrete cover more quickly due to the greater diffusion coefficient.
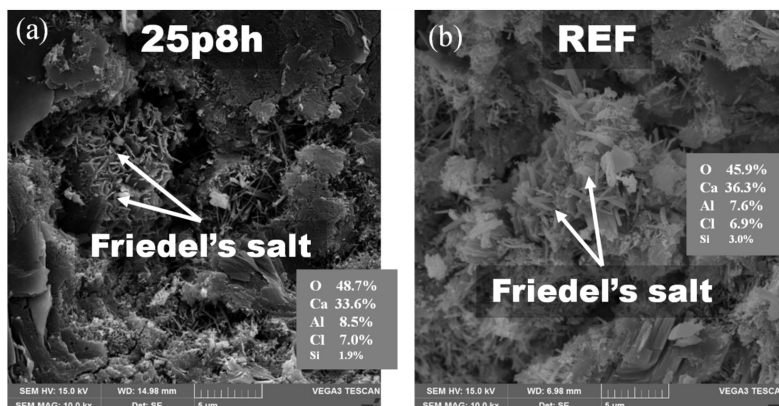

Figure 9. Friedel's salt formation: (a) concrete 25p8h (depth of 25-35 mm); (b) reference concrete (depth of 0-10 mm).

Rev. IBRACON Estrut. Mater., vol. 16, no. 6, e16603, 2023

14/17

4 CONCLUSIONS

The following conclusions were obtained from the execution of this research:

- The effect of CO_2 pressure on chloride profiles was negative and increased with the curing times. The application of 8 hours of curing time was the only one that reduced the chloride profiles to practically all depths, regardless of pressure. Therefore, the combination of less time and pressure during carbonation curing potentiated the reduction of chloride penetration in concrete. There was a tendency for the chloride profiles to become higher than the reference concrete with increasing pressure. Therefore, increasing the CO_2 pressure does not seem to be an adequate solution for the protection of the concrete against the chloride ingress.

- The carbonation curing conditions of 5 and 10 Psi for 8 hours reduced the chloride diffusion coefficient compared to the reference concrete. The concretes cured in the other three pressure levels (15, 20, and 25 Psi) for 8 hours showed diffusion coefficients similar to the reference concrete. However, the estimated chloride surface concentration for all concretes cured for 8 hours in the carbonation chamber was lower than the reference concrete. Thus, the carbonation cure applied over 8 hours was efficient to increase the concrete's resistance to chloride penetration.

- The chloride diffusion coefficients were generally greater (chloride profiles became more horizontal) with increased CO_2 pressure and time. However, the surface chloride concentration of concrete cured by carbonation was lower than the reference concrete. Thus, chlorides had greater difficulty in initially entering concrete cured by carbonation, due to the higher density of the surface layers of the cement matrix. However, chlorides had greater mobility in carbonation-cured concrete at high pressures during the longest times. This behavior was related to the greater difficulty of concrete cured by carbonation to chemically fix chloride ions for the formation of Friedel's salt.

REFERENCES

[1] W. Shi, M. Najimi, and B. Shafei, "Reinforcement corrosion and transport of water and chloride ions in shrinkage-compensating cement concretes," *Cement Concr. Res.*, vol. 135, pp. 106121, Sept. 2020, http://dx.doi.org/10.1016/j.cemconres.2020.106121.

[2] R. A. Medeiros-Junior, "Impact of climate change on the service life of concrete structures," in *Eco-efficient Repair and Rehabilitation of Concrete Infrastructures*, F. Pacheco-Torgal, R. Melchers, N. Belie, X. Shi, K. Van Tittelboom, A.S. Perez, Eds., Duxford, UK: Woodhead Publishing, 2018, pp. 43–68.

[3] X. Xie, Q. Feng, Z. Chen, L. Jiang, and W. Lu, "Diffusion and distribution of chloride ions in carbonated concrete with fly ash," *Constr. Build. Mater.*, vol. 218, pp. 119–125, Sept. 2019, http://dx.doi.org/10.1016/j.conbuildmat.2019.05.041.

[4] R. A. Medeiros-Junior and D. H. Bem, "Study of the environment factor from Fick's and electrical resistivity models by simulation of chloride diffusivity prediction," *Adv. Struct. Eng.*, vol. 23, no. 10, pp. 2097–2109, 2020, http://dx.doi.org/10.1177/1369433220906932.

[5] D. Zhang and Y. Shao, "Effect of early carbonation curing on chloride penetration and weathering carbonation in concrete," *Constr. Build. Mater.*, vol. 123, pp. 516–526, Oct. 2016, http://dx.doi.org/10.1016/j.conbuildmat.2016.07.041.

[6] C. J. Goodbrake, J. F. Young, and R. L. Berger, "Reaction of hydraulic calcium silicates with carbon dioxide and water," *J. Am. Ceram. Soc.*, vol. 62, pp. 488–491, Sept. 1979, http://dx.doi.org/10.1111/j.1151-2916.1979.tb19112.x.

[7] V. Rostami, Y. Shao, A. J. Boyd, and Z. He, "Microstructure of cement paste subject to early carbonation curing," *Cement Concr. Res.*, vol. 42, pp. 186–193, Jan. 2012, http://dx.doi.org/10.1016/j.cemconres.2011.09.010.

[8] D. Zhang and Y. Shao, "Early age carbonation curing for precast reinforced concretes," *Constr. Build. Mater.*, vol. 113, pp. 134–143, June 2016, http://dx.doi.org/10.1016/j.conbuildmat.2016.03.048.

[9] P. He, C. Shi, Z. Tu, C. S. Poon, and J. Zhang, "Effect of further water curing on compressive strength and microstructure of CO_2-cured concrete," *Cement Concr. Compos.*, vol. 72, pp. 80–88, Sept. 2016, http://dx.doi.org/10.1016/j.cemconcomp.2016.05.026.

[10] L. Mo, F. Zhang, and M. Deng, "Mechanical performance and microstructure of the calcium carbonate binders produced by carbonating steel slag paste under CO_2 curing," *Cement Concr. Res.*, vol. 88, pp. 217–226, Oct. 2016., http://dx.doi.org/10.1016/j.cemconres.2016.05.013.

[11] B. J. Zhan, C. S. Poon, and C. J. Shi, "Materials characteristics affecting CO_2 curing of concrete blocks containing recycled aggregates," *Cement Concr. Compos.*, vol. 67, pp. 50–59, Mar. 2016, http://dx.doi.org/10.1016/j.cemconcomp.2015.12.003.

[12] D. Zhang, X. Cai, and Y. Shao, "Carbonation curing of precast fly ash concrete," *J. Mater. Civ. Eng.*, vol. 28, no. 11, pp. 04016127, Nov. 2016, http://dx.doi.org/10.1061/(ASCE)MT.1943-5533.0001649.

[13] S. Ahmad, R. A. Assaggaf, M. Maslehuddin, O. S. B. Al-Amoudi, S. K. Adekunle, and S. I. Ali, "Effects of carbonation pressure and duration on strength evolution of concrete subjected to accelerated carbonation curing," *Constr. Build. Mater.*, vol. 136, pp. 565–573, Apr. 2017, http://dx.doi.org/10.1016/j.conbuildmat.2017.01.069.

[14] Z. Liu and W. Meng, "Fundamental understanding of carbonation curing and durability of carbonation-cured cement-based composites: A review," *J. CO2 Util.*, vol. 44, pp. 101428, Feb. 2021, http://dx.doi.org/10.1016/j.jcou.2020.101428.

[15] L. Qin, X. Gao, A. Su, and Q. Li, "Effect of carbonation curing on sulfate resistance of cement-coal gangue paste," *J. Clean. Prod.*, vol. 278, pp. 123897, Feb. 2021, http://dx.doi.org/10.1016/j.jclepro.2020.123897.

[16] X. Pan, C. Shi, N. Farzadnia, X. Hu, and J. Zheng, "Properties and microstructure of CO_2 surface treated cement mortars with subsequent lime-saturated water curing," *Cement Concr. Compos.*, vol. 99, pp. 89–99, May 2019, http://dx.doi.org/10.1016/j.cemconcomp.2019.03.006.

[17] V. Rostami, Y. Shao, and A. J. Boyd, "Durability of concrete pipes subjected to combined steam and carbonation curing," *Constr. Build. Mater.*, vol. 25, no. 8, pp. 3345–3355, Aug. 2011, http://dx.doi.org/10.1016/j.conbuildmat.2011.03.025.

[18] Q. T. Phung et al., "Effect of limestone fillers on microstructure and permeability due to carbonation of cement pastes under controlled CO_2 pressure conditions," *Constr. Build. Mater.*, vol. 82, pp. 376–390, May 2015, http://dx.doi.org/10.1016/j.conbuildmat.2015.02.093.

[19] T. Chen, X. Gao, "Effect of carbonation curing regime on strength and microstructure of Portland cement paste," *J. CO2 Util.*, vol. 34, pp. 74-86, Dec. 2019, https://doi.org/10.1016/j.jcou.2019.05.034.

[20] D. Zhang and Y. Shao, "Enhancing chloride corrosion resistance of precast reinforced concrete by carbonation curing," *ACI Mater. J.*, vol. 116, pp. 3–12, May 2019., http://dx.doi.org/10.14359/51714461.

[21] L. Qin and X. Gao, "Properties of coal gangue-Portland cement mixture with carbonation," *Fuel*, vol. 245, pp. 1–12, June 2019., http://dx.doi.org/10.1016/j.fuel.2019.02.067.

[22] V. Rostami, Y. Shao, A.J. Boyd, "Carbonation curing versus steam curing for precast concrete production", *J. Mater. Civil Eng.*, vol. 24, n. 9, pp. 1221-1229, Sept., 2012, https://doi.org/10.1061/(ASCE)MT.1943-5533.0000462.

[23] D. Sharma and S. Goyal, "Accelerated carbonation curing of cement mortars containing cement kiln dust: An effective way of CO_2 sequestration and carbon footprint reduction," *J. Clean. Prod.*, vol. 192, pp. 844–854, Aug. 2018, http://dx.doi.org/10.1016/j.jclepro.2018.05.027.

[24] J. H. Seo, S. M. Park, and H. K. Lee, "Evolution of the binder gel in carbonation-cured Portland cement in an acidic medium," *Cement Concr. Res.*, vol. 109, pp. 81–89, July 2018, http://dx.doi.org/10.1016/j.cemconres.2018.03.014.

[25] Y. Liu et al., "Properties and microstructure of concrete blocks incorporating drinking water treatment sludge exposed to early-age carbonation curing," *J. Clean. Prod.*, vol. 261, pp. 121257, July 2020, http://dx.doi.org/10.1016/j.jclepro.2020.121257.

[26] T. Saito, S. Khamhou, T. Yumoto, and N. Otsuki, "Permeability of sulfate ions in cementitious materials containing γ-Ca_2SiO_4 after autoclave curing and accelerated carbonation," *J. Adv. Concr. Technol.*, vol. 9, pp. 223–230, Oct. 2011., http://dx.doi.org/10.3151/jact.9.223.

[27] C. Shi, D. Wang, F. He, and M. Liu, "Weathering properties of CO_2-cured concrete blocks," *Resour. Conserv. Recycling*, vol. 65, pp. 11–17, Aug. 2012, http://dx.doi.org/10.1016/j.resconrec.2012.04.005.

[28] D. Xuan, B. Zhan, and C. S. Poon, "Development of a new generation of eco-friendly "concrete blocks by accelerated mineral carbonation," *J. Clean. Prod.*, vol. 133, pp. 1235–1241, Oct. 2016, http://dx.doi.org/10.1016/j.jclepro.2016.06.062.

[29] M. Liu, S. Hong, Y. Wanga, J. Zhang, D. Hou, and B. Dong, "Compositions and microstructures of hardened cement paste with carbonation curing and further water curing," *Constr. Build. Mater.*, vol. 267, pp. 121724, Jan. 2021, http://dx.doi.org/10.1016/j.conbuildmat.2020.121724.

[30] J. Jang and H. Lee, "Microstructural densification and CO_2 uptake promoted by the carbonation curing of belite-rich Portland cement," *Cement Concr. Res.*, vol. 82, pp. 50–57, Apr. 2016, http://dx.doi.org/10.1016/j.cemconres.2016.01.001.

[31] L. Mo and D. K. Panesar, "Effects of accelerated carbonation on the microstructure of Portland cement pastes containing reactive MgO," *Cement Concr. Res.*, vol. 42, pp. 769–777, June 2012, http://dx.doi.org/10.1016/j.cemconres.2012.02.017.

[32] Associação Brasileira de Normas Técnicas, *Concreto – Procedimento para moldagem e cura de corpos de prova*, ABNT NBR 5738, 2015.

[33] H. El-Hassan, Y. Shao, and Z. Ghouleh, "Effect of initial curing on carbonation of lightweight concrete masonry units," *ACI Mater. J.*, vol. 110, pp. 441–450, July 2013, http://dx.doi.org/10.14359/51685791.

[34] H. El-Hassan and Y. Shao, "Early carbonation curing of concrete masonry units with Portland limestone cement," *Cement Concr. Compos.*, vol. 62, pp. 168–177, Sept. 2015, http://dx.doi.org/10.1016/j.cemconcomp.2015.07.004.

Rev. IBRACON Estrut. Mater., vol. 16, no. 6, e16603, 2023

16/17

[35] M. Abdullahi, J.O. Odigure, A.S. Koyo, A.S. Abdulkareem, "Characterization and predictive reaction model for cement-sand-kaolin composite for CO2 sequestration," *J. CO2 Util.*, vol. 16, pp. 169-181, Dec., 2016, https://doi.org/10.1016/j.jcou.2016.06.008.

[36] Y. Zhang, M. Zhang, and G. Ye, "Influence of moisture condition on chloride diffusion in partially saturated ordinary Portland cement mortar," *Mater. Struct.*, vol. 51, pp. 36, Feb. 2018, http://dx.doi.org/10.1617/s11527-018-1162-7.

[37] Réunion Internationale des Laboratories D'essais de Recherches Sur Les Matériaux Et Les Constructions, "CPC-18, "Measurement of hardened concrete carbonation depth," *Mater. Struct.*, vol. 21, pp. 453–455, Nov. 1988, http://dx.doi.org/10.1007/BF02472327.

[38] Réunion Internationale des Laboratories D'essais de Recherches Sur Les Matériaux Et Les Constructions, "Analysis of total chloride content in concrete," *Mater. Struct.*, vol. 35, pp. 583–585, Nov. 2002, http://dx.doi.org/10.1007/BF02483128.

[39] J. Crank, *The Mathematics of Diffusion*, 1. ed. Grã Bretanha: Oxford University Press, 1970.

[40] C. E. T. Balestra, T. A. Reichert, W. A. Pancera, and G. Savaris, "Chloride profile modeling contemplating the convection zone based on concrete structures present for more than 40 years in different marine aggressive zones," *Constr. Build. Mater.*, vol. 198, pp. 345–358, Feb. 2019, http://dx.doi.org/10.1016/j.conbuildmat.2018.11.271.

[41] C. E. T. Balestra, T. A. Reichert, G. Savaris, W. A. Pansera, and R. A. Medeiros-Junior, "Nondestructive method for estimation of chloride profiles: correlation between electrical resistivity and Holliday-empirical equation," *J. Constr. Eng. Manage.*, vol. 146, pp. 04020119, Oct. 2020, http://dx.doi.org/10.1061/(ASCE)CO.1943-7862.0001907.

[42] Fédération Internationale du Béton, *Model Code for Service Life Design*, CEB-FIB-34, 2006.

[43] Comisión Permanente Del Hormigón, *Instrucción del Hormigón Estructural,* EHE-08, 2010.

[44] J. Liu, M. Ba, Y. Du, Z. He, and J. Chen, "Effects of chloride ions on carbonation rate of hardened cement paste by X-ray CT techniques," *Constr. Build. Mater.*, vol. 122, pp. 619–627, Sept. 2016, http://dx.doi.org/10.1016/j.conbuildmat.2016.06.101.

[45] Y. Gao, J. Zhang, S. Zhang, and Y. Zhang, "Probability distribution of convection zone depth of chloride in concrete in a marine tidal environment," *Constr. Build. Mater.*, vol. 140, pp. 485–495, June 2017, http://dx.doi.org/10.1016/j.conbuildmat.2017.02.134.

[46] H. Chang, S. Um, D. Xie, and P. Wang, "Influence of pore structure and moisture distribution on chloride "maximum phenomenon" in surface layer of specimens exposed to cyclic drying-wetting condition," *Constr. Build. Mater.*, vol. 131, pp. 16–30, Jan. 2017, http://dx.doi.org/10.1016/j.conbuildmat.2016.11.071.

[47] R. Cai et al., "Skin effect of chloride ingress in marine concrete: A review on the convection zone," *Constr. Build. Mater.*, vol. 262, pp. 120566, Nov. 2020, http://dx.doi.org/10.1016/j.conbuildmat.2020.120566.

[48] S. R. Pinto, C. Angulski da Luz, G. S. Munhoz, and R. A. Medeiros-Junior, "Resistance of phosphogypsum-based supersulfated cement to carbonation and chloride ingress," *Constr. Build. Mater.*, vol. 263, pp. 120640, Dec. 2020, http://dx.doi.org/10.1016/j.conbuildmat.2020.120640.

[49] W. Klemm and R. Berger, "Accelerated curing of cementitious systems by carbon dioxide: part I. Portland cement," *Cement Concr. Res.*, vol. 2, pp. 567–576, Sept. 1972, http://dx.doi.org/10.1016/0008-8846(72)90111-1.

[50] J. F. Young, R. L. Berger, and J. Breese, "Accelerated curing of compacted calcium silicate mortars on exposure to CO2," *J. Am. Ceram. Soc.*, vol. 57, pp. 394–397, Sept. 1974, http://dx.doi.org/10.1111/j.1151-2916.1974.tb11420.x.

[51] R. A. Medeiros-Junior, M. G. Lima, P. C. Brito, and M. H. F. Medeiros, "Chloride penetration into concrete in an offshore platform-analysis of exposure conditions," *Ocean Eng.*, vol. 103, pp. 78–87, July 2015, http://dx.doi.org/10.1016/j.oceaneng.2015.04.079.

[52] H. Ye, N. Jin, X. Jin, and C. Fu, "Model of chloride penetration into cracked concrete subject to drying–wetting cycles," *Constr. Build. Mater.*, vol. 36, pp. 259–269, Nov. 2012, http://dx.doi.org/10.1016/j.conbuildmat.2012.05.027.

[53] J. Liu et al., "Understanding the interacted mechanism between carbonation and chloride aerosol attack in ordinary Portland cement concrete," *Cement Concr. Res.*, vol. 95, pp. 217–225, May 2017, http://dx.doi.org/10.1016/j.cemconres.2017.02.032.

[54] J. R. Hino Jr, C. E. T. Balestra, and R. A. Medeiros-Junior, "Comparison of test methods to determine resistance to chloride penetration in concrete: Sensitivity to the effect of fly ash," *Constr. Build. Mater.*, vol. 277, pp. 122265, Mar. 2021, http://dx.doi.org/10.1016/j.conbuildmat.2021.122265.